PHYSICAL REVIEW B VOLUME 49, NUMBER 8 15 FEBRUARY 1994-II

Effects of pressure on the optical absorption and photoluminescence of Wöhler siloxene

S. Ernst, M. Rosenbauer, U. Schwarz, P. Deák,* K. Syassen,
M. Stutzmann, and M. Cardona
Max-Planck-Institut für Festkörperforschung, Heisenbergstrasse 1, 70569 Stuttgart, Germany

(Received 25 August 1993)

We have investigated the effect of hydrostatic pressure ($P \leq 5$ GPa) on optical absorption and photoluminescence spectra of Wöhler siloxene ($Si_6O_3H_6$, as prepared) at $T = 300$ K. The absorption edge energy near 2.75 eV decreases linearly with pressure at a rate of $-30\pm$ 3 meV/GPa. For the position of the maximum of the green luminescence band we find a similar pressure coefficient ($dE/dP = -24 \pm 3$ meV/GPa). The intensity of the green luminescence shows a reversible decrease with increasing pressure. The pressure dependence of interlayer and intralayer lattice constants has been determined by x-ray powder diffraction. The observed changes in optical transition energies are discussed in the framework of a semiempirical quantum-chemical calculation of the electronic structure of siloxene.

I. INTRODUCTION

The discovery of strong visible photoluminescence in porous silicon[1] has stimulated renewed interest in the physical properties of siloxene $[Si_6O_3H_6]$.[2,3] Wöhler siloxene (WS) is the most readily obtained modification of siloxene, discovered by Wöhler in 1863.[4] WS is thought to be derived from the so-called Kautski siloxene[5] by partial OH-H substitution. The crystal structure of Kautski siloxene[6] consists of planes in which the silicon atoms form covalently bonded puckered layers similar to the (111) surface of bulk crystalline silicon. The remaining silicon bonds are alternately saturated by H atoms and OH groups (see Fig. 1, chemical notation $[Si_2H(OH)]_{3n}$). The bonding between the planes takes place through weak van der Waals–type interactions. Thus, WS is expected to represent a two-dimensional form of silicon, with strongly modified electronic properties. The basic structure of WS as described above is only obtained via a topochemical reaction (exchange reaction on interlayers) at low temperatures (0–100 °C). In addition, two other siloxene modifications have been postulated which may result from thermal annealing of WS at about 400 °C.[7] In the chain modification $[Si_2H_2O]_{3n}$ and the ring modification $[Si_6H_6O_3]_n$, oxygen atoms are inserted into the silicon planes giving rise to lower-dimensional backbone polymers. The heat treated WS, assumed to be a mixture of these two hypothetical modifications, shows optical properties similar to those of porous silicon.[8,9]

Wöhler siloxene is a direct-gap material with a gap energy of approximately 2.7 eV at room temperature.[8] The larger optical gap of WS relative to crystalline silicon as well as the direct-gap behavior of WS have recently been the subject of a number of theoretical investigations.[10,2,3] At room temperature or below, WS shows a strong yellow-green photoluminescence. The intensity maximum of this photoluminescence is at 2.3 eV.

In this work we report the dependence on hydrostatic pressure of the near-band-gap optical transitions and lattice parameters of WS. We have measured optical absorption and photoluminescence spectra at room temperature for hydrostatic pressures up to 5 GPa.[11] Similar high-pressure studies of the optical properties of porous silicon have been reported in Refs. 12–14. The direct band

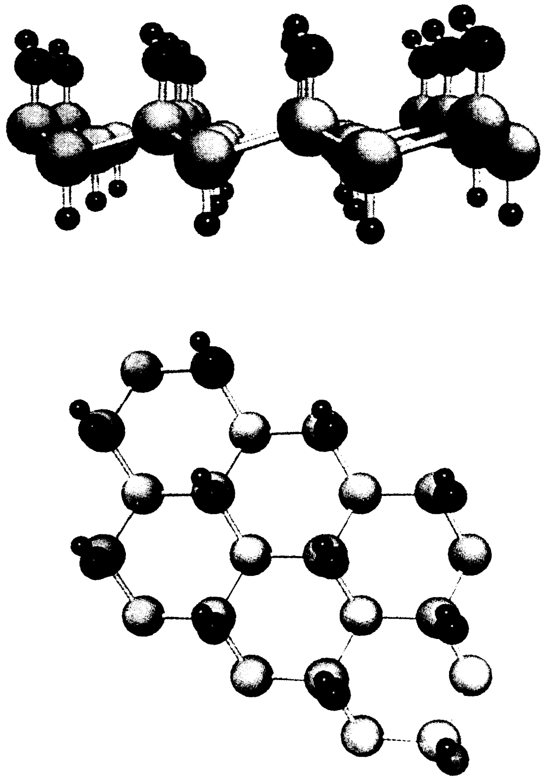

FIG. 1. Structural model of the layers of Wöhler siloxene. The large, medium, and small spheres represent silicon, oxygen, and hydrogen atoms, respectively.

gap of WS is found to show a small reversible redshift with increasing hydrostatic pressure. This behavior is different from that of the *direct* gap of tetrahedrally coordinated semiconductors, which show a strong blueshift of the Γ point gap with increasing pressure[15,16] due to an increase of the bonding-antibonding splitting of the valence- and conduction-band states. Since WS is expected to be a strongly anisotropic material, the change of the interlayer and intralayer lattice constants of WS was determined by powder x-ray diffraction in order to estimate the degree of anisotropy in lattice compression under hydrostatic pressure.

The experimental results for WS are discussed here in the framework of semiempirical quantum-chemical calculations. These calculations were performed for an isolated siloxene layer as well as for two siloxene layers, coupled by weak van der Waals forces.

II. EXPERIMENTAL DETAILS

Wöhler siloxene was synthesized from $CaSi_2$ according to the procedure described elsewhere.[4,7,17] Optical absorption and photoluminescence measurements under hydrostatic pressure were performed in a gasketed diamond anvil cell (DAC) at room temperature. Pressure was measured by the standard ruby luminescence technique. For the absorption measurements samples of homogeneous thickness were prepared by gently pressing a small amount of siloxene powder between the anvils of the DAC. The thickness of the samples is estimated to about 10 μm. In order to avoid chemical reactions between WS and the pressure medium, we have used CsCl (optical absorption) and xenon (photoluminescence) as pressure-transmitting media. This is an important point because of the tendency of the hydrogen ligands of WS to be substituted by other monovalent radicals.[8] This substitution can tune the optical gap over the entire visible spectrum and can also influence the pressure shift of the gap. Also, polar solvents are known to influence the luminescence properties of porous silicon,[18] and similar phenomena could be expected for WS.

For optical absorption white light from a xenon arc lamp was focused onto the sample within the DAC (spot size 30 μm). The transmitted light was dispersed by a 0.64 m monochromator and detected by a photomultiplier coupled to a fast photon counting system. The optical density $D(E)$ was determined by normalizing the transmission through the sample (intensity I) to the transmission through a clear area next to the sample (intensity I_0):

$$D(E) = \log_{10}\frac{I_0(E)}{I(E)}. \tag{1}$$

The determination of the optical density is affected by Rayleigh scattering due to sample inhomogenities. This results in a reduced transmission in the transparent region which varies from run to run. Therefore, absorption spectra were normalized by setting the ratio I/I_0 to 1 at an energy of 2 eV, which is well below the absorption edge energy at all pressures. For photoluminescence measurements the power density of the exciting argon ion laser (488 nm) was always kept below 100 mW/cm^2 in order to avoid photochemical reactions. The luminescence spectra were measured by multichannel detection using a charge coupled device (CCD) detector. Powder x-ray diffraction patterns were measured in an angle-dispersive mode. The diffractometer in Debye-Scherrer geometry was operated with filtered Mo $K\alpha$ radiation. Intensities were recorded using a position-sensitive detection system.

III. EXPERIMENTAL RESULTS

Figure 2 shows absorption spectra measured at different hydrostatic pressures. In this figure we have plotted the optical density versus energy. The linearly increasing background below ≈ 2.7 eV is due to scattering processes. The onset of absorption (at 2.75 eV for zero pressure) is indicated by the change of the slope of the spectrum. The absorption edge energy is defined here as intersection of the linear extrapolations of the background signal and the absorption edge as is illustrated in Fig. 2 for the absorption spectrum at 1.2 GPa.

It is obvious from Fig. 2 that the effect of pressure on the absorption edge energy is extremely small compared to other direct-gap semiconductors. In order to determine the pressure coefficient of the gap energy, we use the shift of the absorption edge at optical density 1 (see Fig. 2). The result is essentially the same if we take the intersection of the two straight lines defining the absorption edge energy, but the scatter of these data points is somewhat larger. The energy of the absorption edge at optical density 1 versus the pressure is shown in Fig. 3

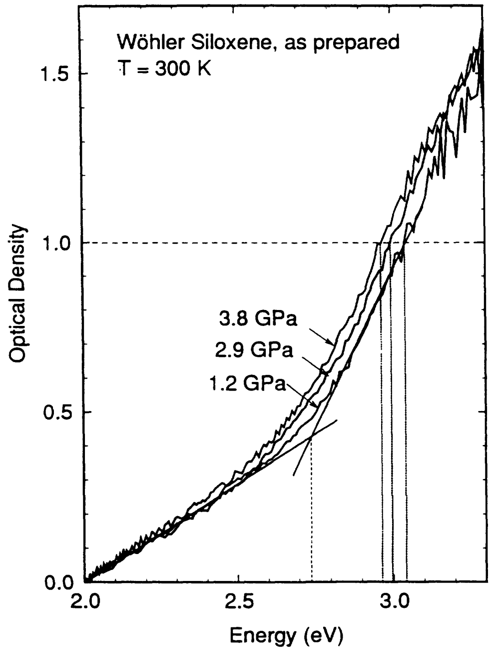

FIG. 2. Optical absorption spectra of Wöhler siloxene. Shown is the optical density versus photon energy. The sample thickness is roughly 10 μm. The absorption edge energy is given by the intersection of the linear extrapolations for background and edge as indicated for the spectrum at 1.2 GPa.

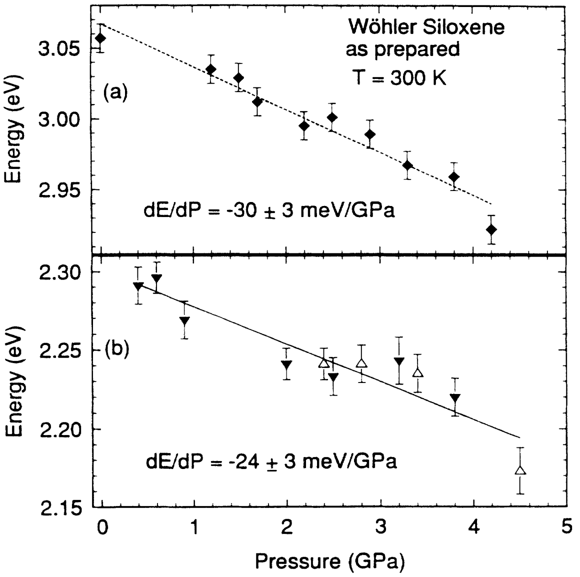

FIG. 3. Pressure dependence of (a) the optical absorption edge at optical density 1 (see Fig. 2) and (b) the photoluminescence maximum of Wöhler siloxene. The pressure effects are reversible as indicated in (b) by open and closed symbols corresponding to increasing and decreasing hydrostatic pressures.

(a). Within experimental uncertainity we find a linear dependence of the absorption edge on pressure with a pressure coefficient of −30 ± 3 meV/GPa.

In the photoluminescence (PL) measurements we observe a broad photoluminescence band with the intensity maximum at 2.3 eV at ambient pressure. Some PL spectra measured at different pressures are shown in Fig. 4. The large statistical fluctuation of the PL signal is due to the fact that an extremely low excitation power was used in order to avoid photochemical reactions. In order to remain below a typical damage threshold of 100 mW/cm^2 the total excitation intensity on the sample (200 μm in diameter) had to be less than 10 μW. In the pressure range from 2.8 up to 4.5 GPa the intensity of the PL signal decreases reversibly by a factor of 2–3. Above 5 GPa the photoluminescence becomes too weak to determine an intensity maximum. The PL maximum shows a small redshift with increasing pressure, as indicated by arrows in Fig. 4. In Fig. 3(b) we have plotted the energy of the photoluminescence maximum versus pressure. The pressure effects are reversible as indicated by open and closed symbols, corresponding to increasing and decreasing hydrostatic pressure. The pressure coefficient for the PL maximum is −24 ± 3 meV/GPa. This is in reasonable agreement with the results of the optical absorption measurements.

Figures 5 (a) and (b) show the pressure dependence of the two lattice distances (*d* values) corresponding to the main peaks which were observed in x-ray diffraction. Zero-pressure values are in good agreement with data given in Refs. 6 and 19. The smaller *d* value [Fig. 5(a)] refers to the (110) reflection and provides information on the relative change of the in-plane lattice constant.

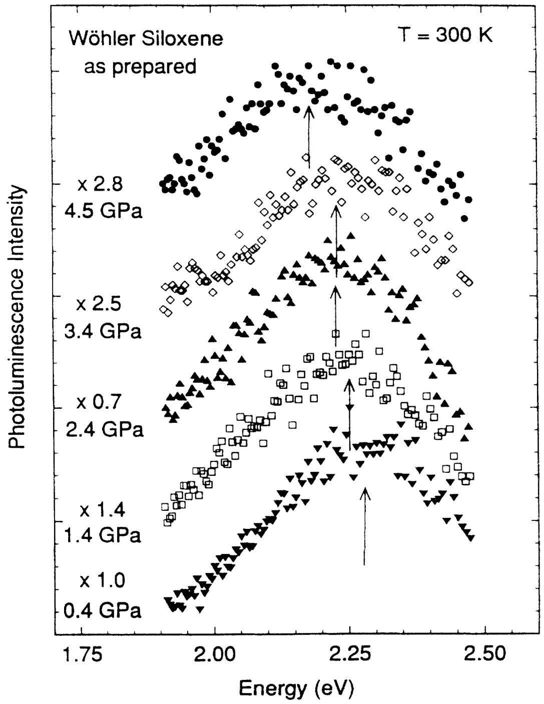

FIG. 4. Room-temperature photoluminescence spectra of WS at selected pressures. The small redshift of the photoluminescence maximum is indicated by arrows. The energies indicated by the arrows were determined from the maxima of second-order polynomials fitted to the spectra near the maximum. The intensity of the PL signal shows a reversible decrease with pressure by a factor of 2–3 between 2.8 GPa and 4.5 GPa. Normalization factors are given for each spectrum.

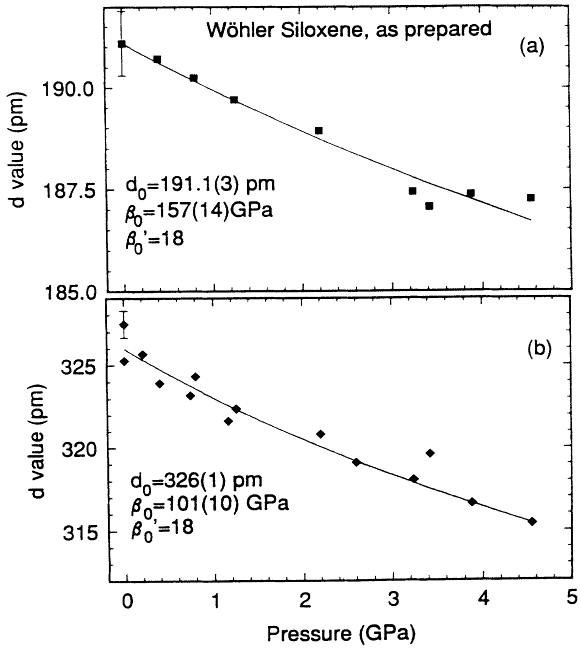

FIG. 5. Pressure dependence of the *d* value of (a) the (110) reflection and (b) the interlayer distance of Wöhler siloxene determined from x-ray powder diffraction.

The larger d value [Fig. 5(b)] corresponds to the (002) reflection (assuming AA stacking of layers) and therefore measures the relative change of the distance between Si layers in WS. The d value versus pressure data were fitted by a Murnaghan-type relation,[20]

$$d(P) = d_0 \left(\frac{P\beta_0'}{\beta_0} + 1 \right)^{1/\beta_0'} , \tag{2}$$

yielding the approximate inverse linear compressibilities β_0 given in Fig. 5. Constant values were assumed for the pressure derivatives $\beta' = d\beta/dP$. The large errors of β_0 are caused by poor signal-to-background ratio of the diffraction patterns and by the admixture of different phases. The linear compressibility of WS is clearly anisotropic and significantly larger compared to crystalline silicon ($\beta_0 = 299.4$ GPa).

IV. CALCULATIONS

In order to understand the effect of hydrostatic pressure on the direct band gap of WS we have to consider several contributions: (i) A decrease of the covalent intralayer Si-Si bonds is expected to cause a blueshift of the direct gap due to an increase of the bonding-antibonding splitting of the near-band-gap states. (ii) Due to the puckering of the WS layers the application of pressure may cause a change in the bond angle, which will also have an effect on the band-gap energy. (iii) Increasing interlayer interaction is expected to result in a redshift of the band gap similar to the behavior of layered semiconductors under pressure.[21,22]

It is not clear *a priori* which of these three effects is dominant. We therefore simulated their influence on the electronic structure of siloxene by performing semiempirical quantum-chemical cyclic cluster calculations. Among numerous calculational methods used by chemists, MINDO/3 (modified intermediate neglect of differential overlap)[23] was long considered to yield the most reliable equilibrium geometries for silicon[24] and SiO_2.[25] On the other hand the Austin model (AM1) is expected to be more precise in predicting bond strengths and force constants.[10] When external pressure is applied, however, nothing is known so far about the reliability of these different methods.

Therefore, in a first step, the applicability of MINDO/3 and AM1 to Si under hydrostatic pressure was tested for a Si_{32} cluster at different lattice constants. In this case, the energy change

$$\Delta E = \frac{1}{2} \sum_{i=1}^{N} k_r (r \Delta r_i)^2 , \tag{3}$$

under pressure is the elastic energy of the N Si-Si bonds which are compressed by a change in bond length of Δr_i. Using MINDO/3, we found for the spring constant k_r = 235 N/m. AM1 gives 209 N/m, while the experimental value is 152 N/m.[26] As expected, AM1 is more reliable in Si under hydrostatic pressure.

Since the quantum-chemical methods were parametrized for chemical bonds, we cannot expect them to give very good results for the interlayer interactions. We therefore consider the effects within the planes first. Using AM1, we calculated the change of the geometry and the total energy of a $(Si_6O_3H_6)_3$ siloxene cluster when varying the in-plane lattice constant between 101% and 95% of the calculated equilibrium value (3.82 Å).

In a first series of calculations, the only restriction we imposed on the geometry was the value of the lattice constant, i.e., we allowed both bond-angle and bond-length variations. In order to enable a comparison with the experimental results, we determined the pressure numerically from the relation

$$P = -\left(\frac{\partial F}{\partial V} \right)_T \approx -\left(\frac{\partial E}{\partial V} \right)_T . \tag{4}$$

The total energy E in Eq. (4) was calculated as the sum of two contributions: (i) the theoretical energy due to deformation of bond angles and bond lengths within the two-dimensional Si planes, and (ii) the energy required to bring adjacent Si planes closer together. This energy was deduced from the experimental results in Fig. 5. The theoretical pressure necessary for a compression of the in-plane lattice constant a to 98% was obtained to be 5.9 GPa. This is fairly close to the experimental value of 4.0 GPa.

For the calculations of the electronic structure and optical transitions, the CNDO/S (complete neglect of differential overlap) method has proven to give useful results for electronic spectra of molecules. CNDO/S has been parametrized[27] to reproduce the spectra of large saturated molecules of C, O, H, and Si. Using the geometries obtained from the AM1 calculations as input for the CNDO/S program, we calculated the electronic structure and the lowest optical transition using a limited CI (configuration interaction) with 144 single excited configurations for several geometries. The results are shown in Fig. 6.

The calculated redshift for a deformation (variation of bond length *and* bond angle) to 98% is 80 meV compared to a 120 meV (96 meV) redshift measured experimentally for the absorption (luminescence) spectrum. The difference between theory and experiment is most likely due to the neglected change of the electronic structure when the planes are brought closer together (see below).

In a second series of calculations, we tried to separate the effect of bond length variations from that due to changes in the bond angle. We kept the Si-Si-Si bond angles fixed and only allowed a change in the Si-Si bond lengths when reducing the lattice constant. The resulting optical transitions (see Fig. 6) show a blueshift of 90 meV when compressing the planes to 98% of their original size. Analyzing the change in total energy under these conditions via Eq. (3), we find a spring constant in siloxene of k_r = 204 N/m, which is very close to the value obtained for crystalline silicon.

Alternatively, we kept the Si-Si bond lengths fixed and only allowed a change in the Si-Si-Si bond angles, i.e., a change in the corrugation of the planes when reducing the lattice constant. The increased interaction of the silicon atoms with their second neighbors is expected to result in a broadening of the bands and therefore in a reduced

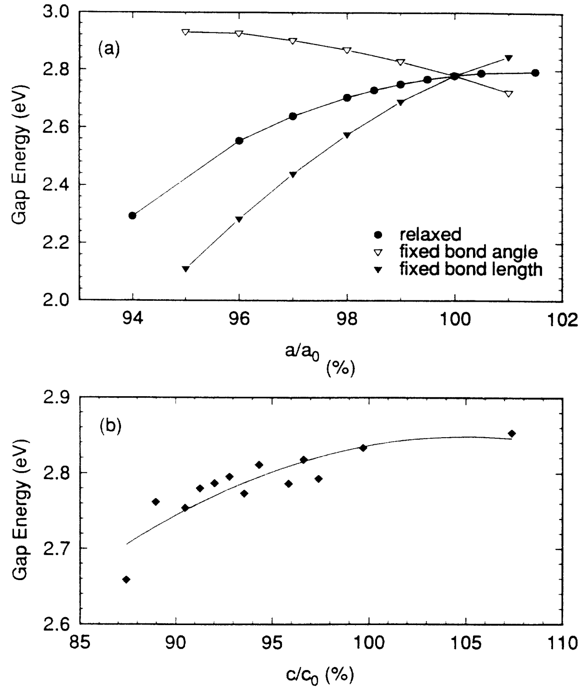

FIG. 6. Calculated effect of hydrostatic pressure on the optical transition energy for (a) an isolated siloxene layer (cluster size $n = 3$) with relaxed geometry (●), fixed bond length and relaxed bond angle (▼), and fixed bond angle and relaxed bond length (▽). (b) shows the variation of optical transition energies for two layers (two $n = 3$ clusters) due to changes in interlayer coupling.

band gap. The calculated redshift for a compression to 98% (Fig. 6) is 200 meV. These calculations can also be used to obtain an approximate value for the bond-bending spring constant k_θ defined by[26]

$$\Delta E = \frac{1}{2}\sum_{i=1}^{M} k_\theta \,(\Delta\theta_i)^2, \qquad (5)$$

where M is the total number of Si bond angles in the cluster. Calculating the average value for $|\Delta\theta_i|$ of the six bond angles at each Si atom and relating it to the increase in the total energy, we find a bond-bending spring constant of $k_\theta = 6.4$ N/m in siloxene, compared to the experimentally determined spring constant for crystalline silicon of $k_\theta = 9.2$ N/m.[26]

To estimate the effect of the decreased interplanar distance on the electronic structure, we finally calculated the optical transitions of a $(\mathrm{Si_6O_3H_6})_6$ cluster which consisted of two parallel siloxene planes which were stacked one above the other without displacement (*AA* stacking). AM1 was used to find the most energetically favorable bond angles and bond lengths for the OH and H ligands. The Si-Si bond lengths and bond angles were kept fixed. For the experimentally determined change of $\Delta c = -0.2$ Å, the calculations predict an additional redshift of about 20 meV [see Fig. 6(b)]. Therefore, we obtain from the calculations a total pressure coefficient of -25 meV/GPa. This pressure coefficient is in excellent agreement with the experimental pressure coefficient.

V. SUMMARY

We have investigated the behavior of Wöhler siloxene under high pressure by optical spectroscopy and powder x-ray diffraction for pressures up to 5 GPa. From x-ray diffraction experiments we find that WS is more compressible (compared to crystalline Si), not only in the direction perpendicular to the layers, but also within the layers. On the other hand, the application of hydrostatic pressure results only in a small reversible redshift (about -27 meV/GPa) of the near-band-gap optical transition energies in Wöhler siloxene. Results of photoluminescence and optical absorption measurements are found to be consistent, if care is taken to avoid chemical reactions with the pressure medium. Semiempirical quantum-chemical calculations (AM1 and CNDO/S-CI) predict a redshift of the band gap of -25 meV/GPa in excellent agreement with experiment. Based on the quantum-chemical calculations the small redshift of the band gap under pressure can be attributed to three different contributions: The decrease of the nearest-neighbor Si-Si bond-length results in a blueshift of the band gap as a consequence of the increasing bonding-antibonding splitting of the covalent in-plane bonds. This effect is nearly compensated by a redshift arising from an increased puckering of the layers (change of Si-Si-Si bond angle) with increasing pressure. The increase of the interlayer coupling due to pressure causes an additional redshift of the band gap. The experimental data and the calculations indicate that at all pressures there is an approximate cancellation of the effects arising from nearest-neighbor Si-Si covalent bonding and second-nearest-neighbor as well as interlayer coupling.

ACKNOWLEDGMENTS

The theoretical part of this work was supported by the European Community under PECO Project No. 7839.

---

[*] Also at Technical University, Budapest H-1521, Hungary.

[1] L. T. Canham, Appl. Phys. Lett. **57**, 1046 (1990).
[2] C. G. Van de Walle and J. E. Northrup, Phys. Rev. Lett. **70**, 1116 (1993).
[3] K. Takeda and K. Shiraishi, Solid State Commun. **85**, 301 (1993).
[4] F. Wöhler, Lieb. Ann. **127**, 275 (1863).
[5] H. Kautsky and H. Zocher, Z. Phys. **9**, 267 (1929).
[6] A. Weiss, G. Beil, and H. Meyer, Z. Naturforsch. B **34**, 25 (1979).
[7] M. Stutzmann, J. Weber, M. S. Brandt, H. D. Fuchs, M. Rosenbauer, P. Deak, A. Höpner, and A. Breitschwerdt, Adv. Solid State Phys. **32**, 179 (1992).
[8] M. Stutzmann, M. S. Brandt, H. D. Fuchs, M. Rosenbauer,

M. K. Kelly, P. Deák, J. Weber, and S. Finkbeiner, in *Optical Phenomena in Semiconductor Structures of Reduced Dimensions,* edited by D. J. Lockwood and A. Pinczale (Kluwer, Dordrecht, 1993), p. 427.

[9] M. Stutzmann, M. S. Brandt, M. Rosenbauer, J. Weber, and H. D. Fuchs, Phys. Rev. B **47**, 4806 (1993).

[10] P. Deák, M. Rosenbauer, M. Stutzmann, J. Weber, and M. S. Brandt, Phys. Rev. Lett. **69**, 2531 (1992).

[11] A preliminary report was given in H. D. Fuchs, M. Rosenbauer, M. S. Brandt, S. Ernst, S. Finkbeiner, M. Stutzmann, K. Syassen, J. Weber, H. J. Queisser, and M. Cardona, in *Microcrystalline Semiconductors: Materials, Science, and Devices*, edited by P. M. Vochet, C. C. Tsai, L. T. Canham, E. Shimizu, and Y. Aoyagi, MRS Symposia Proceedings No. 283 (Materials Research Society, Pittsburgh, 1993), p. 203.

[12] W. Z. Zhou, H. Shen, J. F. Harvey, R. A. Lux, M. Dutta, F. Lu, C. H. Perry, R. Tsu, N. M. Kalkhoran, and F. Namavar, Appl. Phys. Lett. **61**, 1435 (1992).

[13] A. K. Sood, K. Jayaram, D. Victor, and S. Muthu, J. Appl. Phys. **72**, 4963 (1992).

[14] J. Camassel, E. Massone, S. Lyapin, J. Allegre, P. Vicente, A. Foucaran, A. Raymond, and J. L. Robert, in *Proceedings of the 21st International Conference on the Physics of Semiconductors, Beijing, 1992*, edited by Ping Jiang and Hou-Zhi Zheng (World Scientific, Singapore, 1992), p. 1463.

[15] D. L. Camphausen, G. A. N. Connell, and W. Paul, Phys. Rev. Lett. **26**, 184 (1971).

[16] For experimental values see, *Crystal and Solid State Physics*, Landolt-Börnstein, New Series, Group III, Vol. 17, edited by O. Madelung, M. Schulz, and H. Weiss, Part A (Springer-Verlag, Heidelberg, 1982); *Crystal and Solid State Physics*, Landolt-Börnstein, New Series, Group III, Vol. 22, Part A, edited by O. Madelung and M. Schulz (Springer-Verlag, Heidelberg, 1987).

[17] M. S. Brandt, H. D. Fuchs, M. Stutzmann, J. Weber, and M. Cardona, Solid State Commun. **81**, 307 (1992).

[18] J. M. Lauerhaas, G. M. Credo, J. L. Heinrich, and M. J. Sailor, in *Light Emission from Silicon*, edited by S. S. Iyer, R. T. Collins, and L. T. Canham (Materials Research Society, Pittsburgh, 1992), p. 137.

[19] J. R. Dahn, B. M. Way, and E. Fuller (unpublished).

[20] F. D. Murnaghan, Proc. Natl. Acad. Sci. **44**, 244 (1944).

[21] M. Gauthier, A. Polian, J. M. Besson, and A. Chevy, Phys. Rev. B **40**, 3837 (1989).

[22] A. R. Goñi, A. Cantarero, U. Schwarz, K. Syassen, and A. Chevy, Phys. Rev. B **45**, 4221 (1992).

[23] R. C. Bingham, M. J. S. Dewar, and D. H. Lo, J. Am. Chem. Soc. **97**, 1285 (1975).

[24] P. Deák and L. Snyder, Phys. Rev. B **36**, 9619 (1987).

[25] A. H. Eduards and W. B. Fowler, J. Phys. Chem. Solids **46**, 841 (1985).

[26] R. M. Martin, Phys. Rev. B **1**, 4005 (1970).

[27] P. Deák, Int. J. Quantum Chem. **23**, 1156 (1983).

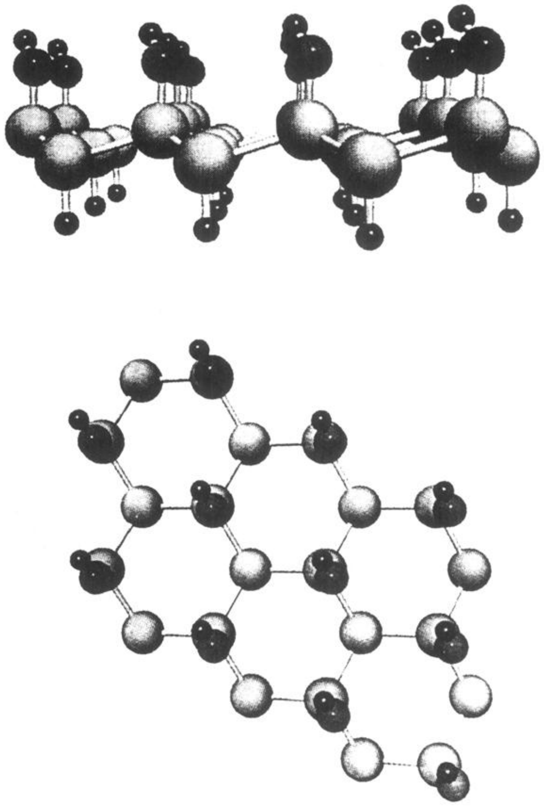

FIG. 1. Structural model of the layers of Wöhler siloxene. The large, medium, and small spheres represent silicon, oxygen, and hydrogen atoms, respectively.